



## ORIGINAL ARTICLE

*ATP5H/KCTD2* locus is associated with Alzheimer's disease risk

M Boada<sup>1,2,15</sup>, C Antúnez<sup>3,15</sup>, R Ramírez-Lorca<sup>4,15</sup>, AL DeStefano<sup>5,6</sup>, A González-Pérez<sup>4</sup>, J Gayán<sup>4</sup>, J López-Arrieta<sup>7</sup>, MA Ikram<sup>8</sup>, I Hernández<sup>1</sup>, J Marín<sup>3</sup>, JJ Galán<sup>4</sup>, JC Bis<sup>9</sup>, A Mauleón<sup>1</sup>, M Rosende-Roca<sup>1</sup>, C Moreno-Rey<sup>4</sup>, V Gudnasson<sup>10</sup>, FJ Morón<sup>4</sup>, J Velasco<sup>4</sup>, JM Carrasco<sup>4</sup>, M Alegret<sup>1</sup>, A Espinosa<sup>1</sup>, G Vinyes<sup>1</sup>, A Lafuente<sup>1</sup>, L Vargas<sup>1</sup>, AL Fitzpatrick<sup>9</sup>, for the Alzheimer's Disease Neuroimaging Initiative<sup>16</sup>, LJ Launer<sup>11</sup>, ME Sáez<sup>4</sup>, E Vázquez<sup>4</sup>, JT Becker<sup>12</sup>, OL López<sup>12</sup>, M Serrano-Ríos<sup>13</sup>, L Tárrega<sup>1</sup>, CM van Duijn<sup>8</sup>, LM Real<sup>4</sup>, S Seshadri<sup>5,6,14</sup> and A Ruiz<sup>1,4</sup>

To identify loci associated with Alzheimer disease, we conducted a three-stage analysis using existing genome-wide association studies (GWAS) and genotyping in a new sample. In Stage I, all suggestive single-nucleotide polymorphisms (at  $P < 0.001$ ) in a previously reported GWAS of seven independent studies (8082 Alzheimer's disease (AD) cases; 12 040 controls) were selected, and in Stage II these were examined in an *in silico* analysis within the Cohorts for Heart and Aging Research in Genomic Epidemiology consortium GWAS (1367 cases and 12904 controls). Six novel signals reaching  $P < 5 \times 10^{-6}$  were genotyped in an independent Stage III sample (the Fundació ACE data set) of 2200 sporadic AD patients and 2301 controls. We identified a novel association with AD in the adenosine triphosphate (ATP) synthase, H<sup>+</sup> transporting, mitochondrial F0 (*ATP5H*)/Potassium channel tetramerization domain-containing protein 2 (*KCTD2*) locus, which reached genome-wide significance in the combined discovery and genotyping sample (rs11870474, odds ratio (OR) = 1.58,  $P = 2.6 \times 10^{-7}$  in discovery and OR = 1.43,  $P = 0.004$  in Fundació ACE data set; combined OR = 1.53,  $P = 4.7 \times 10^{-9}$ ). This *ATP5H/KCTD2* locus has an important function in mitochondrial energy production and neuronal hyperpolarization during cellular stress conditions, such as hypoxia or glucose deprivation.

*Molecular Psychiatry* (2014) **19**, 682–687; doi:10.1038/mp.2013.86; published online 16 July 2013

**Keywords:** Alzheimer's disease; genomics; GWAS; molecular epidemiology; SNP

## INTRODUCTION

Alzheimer's disease (AD) is the most common cause of dementia. It is expected that AD prevalence will be quadrupled by 2040, reaching a worldwide number of 81.1 million affected individuals.<sup>1</sup> In spite of the knowledge that genetic factors may account for about 60–80% of AD susceptibility,<sup>2</sup> the *APOE* epsilon 4 allele was, until very recently, the only accepted risk factor for late-onset AD (LOAD).<sup>3</sup> Fortunately, genome-wide association study (GWAS) technologies are rapidly transforming our knowledge of susceptibility factors related to LOAD. Specifically, in the past three years, nine additional loci located in or adjacent to clusterin (*CLU*), *PICALM*, *CR1*, *BIN1*, the *MS4A* gene cluster, *ABCA7*, *EPHA1*, *CD33* and *CD2AP*, have been identified.<sup>4–9</sup> There is no obvious relationship between the most of these novel loci and the current models of the pathogenesis of AD (that is, the amyloid and tau hypotheses), rather the novel genes identified point to immune system function, cholesterol metabolism and synaptic cell membrane processes as

important in determining the risk of LOAD.<sup>10</sup> However, researchers are intensively looking for direct relationships between these novel loci and amyloid deposition speculating that new genes might have effects on amyloid metabolism or through previously unsuspected pathophysiological pathways, and indeed preliminary evidence for relationships between the amyloid hypothesis and some of the novel loci is rapidly emerging.<sup>11</sup>

Specifically, it has been reported that *PICALM* has a role in beta-amyloid membrane trafficking in yeast models;<sup>11</sup> Furthermore using highly sensitive single-molecule fluorescence methods, Narayan *et al.*<sup>12</sup> have established a direct link between the *CLU* protein and beta-amyloid toxicity, observing that beta amyloid forms a heterogeneous group of small oligomers (from dimers to 50-mers), all of which interact with the sequestering *clu* protein to form long-lived complexes.<sup>12</sup>

Overall, the known loci explain only a small fraction of the known heritability of polygenic AD. In this paper, we present the

<sup>1</sup>Memory Clinic of Fundació ACE, Institut Català de Neurociències Aplicades, Barcelona, Spain; <sup>2</sup>Hospital Universitari Vall d'Hebron–Institut de Recerca, Universitat Autònoma de Barcelona (VHIR-UAB), Barcelona, Spain; <sup>3</sup>Dementia Unit, University Hospital Virgen de la Arrixaca, Murcia, Spain; <sup>4</sup>Department of Structural Genomics, Neocodex, Sevilla, Spain; <sup>5</sup>Department of Neurology Boston University School of Medicine, Boston, MA, USA; <sup>6</sup>Department of Biostatistics, Boston University School of Medicine, Boston, MA, USA; <sup>7</sup>Memory Unit, University Hospital La Paz-Cantoblanco, Madrid, Spain; <sup>8</sup>Department of Epidemiology, Erasmus MC University Medical Center, Rotterdam, The Netherlands; Netherlands Consortium for Healthy Aging, Leiden, The Netherlands; <sup>9</sup>Department of Medicine, University of Washington, Seattle, WA, USA; <sup>10</sup>Icelandic Heart Association, Kopavogur University of Iceland, Kopavogur, Iceland; <sup>11</sup>Laboratory of Epidemiology, Demography, and Biometry, Intramural Research Program, National Institute on Aging, Washington, DC, USA; <sup>12</sup>Alzheimer's Disease Research Center, Departments of Neurology, Psychiatry and Psychology, University of Pittsburgh School of Medicine, Pittsburgh, PA, USA; <sup>13</sup>Centro de Investigación Biomédica en Red de Diabetes y Enfermedades Metabólicas Asociadas (CIBERDEM) Spain, Hospital Clínico San Carlos, Madrid, Spain and <sup>14</sup>National Heart, Lung and Blood Institute's Framingham Heart Study, Framingham, MA, USA. Correspondence: Dr A Ruiz, CSO-cap de recerca, Fundació ACE, Institut Català de Neurociències Aplicades, Marqués de Sentmenat 57, Barcelona 08029, Spain.

E-mail: [aruiz@fundacioace.com](mailto:aruiz@fundacioace.com)

<sup>15</sup>The first three authors contributed equally to this work.

<sup>16</sup>Data used in preparation of this article were obtained from the Alzheimer's Disease Neuroimaging Initiative (ADNI) database ([adni.loni.ucla.edu](http://adni.loni.ucla.edu)). As such, the investigators within the ADNI contributed to the design and implementation of ADNI and/or provided data but did not participate in analysis or writing of this report. A complete listing of ADNI investigators can be found at: [http://adni.loni.ucla.edu/wp-content/uploads/how\\_to\\_apply/ADNI\\_Acknowledgement\\_List.pdf](http://adni.loni.ucla.edu/wp-content/uploads/how_to_apply/ADNI_Acknowledgement_List.pdf).

Received 20 April 2012; revised 25 May 2013; accepted 30 May 2013; published online 16 July 2013

results of a collaborative effort to identify additional AD genes. We followed up on all suggestive ( $P < 0.001$ ) results in our previously published GWAS (Stage I) with *in silico* analysis using unpublished data from a previously reported GWAS in the Cohorts for Heart and Aging Research in Genomic Epidemiology (CHARGE) consortium (Stage II). Six novel single-nucleotide polymorphisms (SNPs) that reached a  $P < 5 \times 10^{-6}$  were genotyped in an independent data set (Stage III). This sequential analysis and novel genotyping allowed us to identify a new AD locus (adenosine triphosphate (ATP) synthase, H<sup>+</sup> transporting, mitochondrial F0/Potassium channel tetramerization domain-containing protein 2 (ATP5H/KCTD2) at 17q25.1.

## PATIENTS AND METHODS

### Setting and participants

**Stage I meta-GWAS.** We followed up the results obtained in our initial meta-analysis described previously.<sup>9</sup> Briefly, we undertook GWAS on a sample of 319 sporadic AD patients diagnosed with possible or probable AD and 801 population-based controls.<sup>13</sup> Due to the limited power of our sample to detect small genetic effects, we combined our data with the individual level data from four other publicly available GWAS: TGEN (Translational Genomics Research Institute; 757 cases and 468 controls),<sup>14</sup> ADNI (Alzheimer Disease Neuroimaging Initiative; 164 cases and 194 controls),<sup>15</sup> genADA (Genotype-Phenotype Alzheimer's disease Associations; 782 cases and 773 controls),<sup>16</sup> and NIA (Late Onset Alzheimer's Disease and National Cell Repository for Alzheimer's Disease Family Study: Genome-Wide Association Study for Susceptibility Loci; 987 cases and 802 controls),<sup>17</sup> applying identical quality control filters and the same imputation methods to each data set and undertook a meta-analysis (for details see reference<sup>9</sup>). We also incorporated into this meta-analysis aggregated genotype data from the Pfizer GWAS (Hu *et al.*;<sup>18</sup> 1034 AD cases and 1186 controls) and the GERAD (Genetic and Environmental Risk in AD) consortium GWAS (Harold *et al.*;<sup>4</sup> 3938 AD cases and 7848 controls). For details, see Supplementary Figure S1.

**Stage II: *in silico* analysis in the CHARGE consortium.** We then undertook an *in silico* analysis of suggestive hits identified at Stage I in the CHARGE consortium data set. The analytic strategies for AD GWAS used by CHARGE have been published previously.<sup>5</sup> Briefly, the CHARGE consortium currently includes large, prospective, community-based cohort studies that have GWAS data coupled with extensive data on multiple neurological and non-neurological phenotypes. A neurology working-group arrived at a consensus on phenotype harmonization, covariate selection and analytic plans for within-study analyses followed by meta-analysis of results.<sup>5</sup> Informed consent was obtained from all the participants at entry into the study, and the study protocols were approved by institutional review. Overall, 1367 AD cases (973 incident) and 12 904 controls from CHARGE were included in Stage II analysis.

**Stage III: *de novo* genotyping in the Fundació ACE data set.** The Fundació ACE data set consisted of 4501 individuals: 2200 possible or probable AD patients diagnosed by neurologists<sup>13</sup> and 2301 healthy controls. The controls were selected from a Spanish general population available at the Neocodex bio-bank.<sup>19</sup> An additional 122 neurologically healthy controls were recruited from Fundació ACE as previously described.<sup>20</sup> The AD cases were consecutive patients examined at three recruiting centers: 2032 from Fundació ACE, Institut Català de Neurociències Aplicades (Barcelona, Catalonia, Spain), 161 from Unidad de Memoria, Hospital Universitario La Paz-Cantoblanco (Madrid, Spain) and 7 from Unidad de Demencias, Hospital Universitario Virgen de la Arrixaca (Murcia, Spain). None have genome-wide genotype data available.

In order to avoid population stratification issues, both cases and controls were selected to be of white Mediterranean ancestry with registered Spanish ancestors (for two generations). Demographic characteristics of the Fundació ACE data set are reported in Supplementary Table S1. Written informed consent was obtained from all the individuals included or their representatives when necessary. The referral centers' ethics committees have approved this research protocol that is in compliance with national legislation and the Code of Ethical Principles for Medical Research Involving Human Subjects of the World Medical Association.

### Methods

***In silico* analyses and selection of SNPs for genotyping follow-up.** The procedure to select candidate SNPs is detailed in Supplementary Figure S1. Briefly, we designed a multi-stage strategy to prioritize SNPs for further *de novo* genotyping in the Fundació ACE data set. In the first stage, we selected a relatively large number of SNPs by establishing a permissive cutoff in our original meta-GWAS ( $P < 0.001$ ).<sup>9</sup> A total of 1202 SNPs met this threshold, and results for these SNPs were meta-analyzed with results from the CHARGE GWAS. Thirty-five SNPs with  $P < 5 \times 10^{-6}$  in the joint analysis were selected for follow-up and mapped in the UCSC genome browser.<sup>21</sup> Twenty-eight SNPs located within known AD loci were excluded. Seven novel SNPs reaching a predetermined suggestive  $p$ -value ( $P < 5 \times 10^{-6}$ ) but outside known loci were selected for the final genotyping step in the Fundació ACE data set. Of note, based on 1000 genomes data, we observed that two markers (rs2896209 and rs4406992) were physically close and displayed strong linkage disequilibrium (LD; 20 bp distance,  $r^2 = 0.950$ ). We decided to analyze only one of them. Consequently, the rs2896209 SNP within *SLC24A4* locus was excluded due to strong LD with and close proximity to the rs4406992 marker (Supplementary Figure S1). So, we finally selected six SNPs within new candidate regions for further follow-up. The sample size, the effective sample size, the data sets that were informative and the genotype status (imputed or genotyped) for each selected marker are detailed in Supplementary Table S2.

**Genotyping.** Selected candidate SNPs were genotyped in the Fundació ACE data set using real-time PCR coupled to fluorescence resonance energy transfer. Briefly, we extracted DNA using Magpure technology (Roche Diagnostics, Mannheim, Germany). Of note, all samples were centralized and processed in the same location (Neocodex DNA Laboratory, Seville, Spain). Identical DNA extraction methods, quality controls, equipment and personnel were applied for the entire genotyping project. Primers and probes designed for genotyping protocols are summarized in Supplementary Table S3. The protocols were performed in the LightCycler 480 System instrument (Roche Diagnostics). PCR reactions were performed in a final volume of 20  $\mu$ l using 20 ng of genomic DNA, 0.5  $\mu$ M of each amplification primer, 0.20  $\mu$ M of each detection probe and 4  $\mu$ l of LC480 Genotyping Master 5X (Roche Diagnostics). We used an initial denaturation step of 95 °C for 5 min, followed by 45 cycles of 95 °C for 30 s, 56 °C for 30 s and 72 °C for 30 s. Melting curves were 95 °C for 2 min (ramping rate 4.4 °C s<sup>-1</sup>), 45 °C for 30 s (ramping rate of 1 °C s<sup>-1</sup>) and 70 °C for 0 s (ramping rate of 0.15 °C s<sup>-1</sup>). In the last step of each melting curve, a continuous fluorimetric register was performed by the system at one acquisition register per each degree Celsius. Melting peaks and genotype calls were obtained by using the LightCycler480 software (Roche). In order to confirm genotypes, selected PCR amplicons were bi-directionally sequenced using standard capillary electrophoresis techniques.

**Statistical analysis.** Association analyses in Stage I were carried out using an allelic association test model with no covariates, as implemented in the software Plink (<http://pngu.mgh.harvard.edu/~purcell/plink>), to obtain unadjusted estimates of the effect size and  $P$ -values.<sup>22</sup> We selected SNPs only from the autosomal chromosomes. X, Y and mitochondrial SNPs were excluded. The filters for genotyping completeness, imputation quality, minor allele frequency have been described previously.<sup>9</sup> Briefly, SNPs were selected to have a call rate > 95% (in each case, control and combined group, within each data set), and a minor allele frequency > 1% (again in each case, control and combined group, within each data set). SNPs that deviated grossly from Hardy-Weinberg equilibrium ( $P$ -value <  $10^{-4}$ ) in control samples were removed. We also removed SNPs with a significantly different rate of missingness ( $P$ -value <  $5 \times 10^{-4}$ ) between case and control samples within each data set.

Meta analyses in Stages I, II and III were conducted using inverse variance method (fixed effects model) and random effects model in PLINK's 'meta' option.<sup>22</sup> We presented random effects meta-analysis results only when heterogeneity was observed ( $Q$ -test was statistically significant). The original GWAS in Stage I were treated as separate studies, CHARGE GWAS results were treated as a single additional study. The weighting of each study was calculated using the estimated s.e. Genome-wide significant and highly suggestive  $p$ -value thresholds were established at  $P < 5 \times 10^{-8}$  and  $P < 5 \times 10^{-6}$ , respectively.

Final meta-analysis results and Forest plot for rs11870474 showing association results in the original meta-GWAS, the CHARGE data and the Fundació ACE data set were derived using the Stata 10.0 (College Station, TX, USA) 'metan' command. Global  $p$ -values were calculated in different ways using PLINK or Episheet software (academic software non-commercial).

Multivariate logistic regression models were used to adjust the effect estimates for our top SNP, rs11870474, using age, sex and/or principal components (PCs) and the presence of *APOE* E4 as covariates in data sets wherein these data were available. These analyses were conducted in SPSS 18.0 software (IBM, Armonk, NY, USA) evaluating a dominant model for the minor allele (CC vs CA + AA genotypes).

Power calculations were done with Episheet spreadsheet (<http://www.drugapi.org/links/downloads/episheet.xls>). The basic idea was to calculate minimum sample size necessary to have 80% power to detect a moderate effect of rs11870474 SNP assuming  $z$ -alpha = 1.96, case/control ratio = 1, exposure prevalence 3% and different odds ratio (OR) effects (1.43 and 1.53).

Graphical Representation of Relationships (GRR) software was used to estimate identity by state (IBS) mean values in all individual pairs and visualize the resulting relationships. Any potential duplication or cryptic relatedness across samples was also explored using PLINK or GRR.<sup>23</sup> Individual IBS mean values were calculated to identify samples with common ancestors. In Murcia data set, we found two possible sibling pairs (IBS 1.63–1.67), and one possible second-degree pair (IBS 1.50), while the remaining individuals represented a cluster of diverse ranges of relatedness. Therefore, three individuals were removed to eliminate these relationships. We also found two possible pairs of first-degree relatives (IBS = 1.63–1.70) in the ADNI data set, who were also removed from the analysis. We do not need to remove any subject from the NIA, TGEN or GenADA studies (IBS < 1.50 in all individuals). However, when relatedness was explored across these databases, we detected 15 samples that might be duplicated and 6 related individuals. These were patients from the Mayo clinic (TGEN), GenADA and ADNI data sets who had also been included in the NIA GWAS (Supplementary Table S12). The potential impact of this unexpected finding, undetected in our previous report, was evaluated separately. In fact, after removing detected duplications we re-calculated effect sizes and *P*-values that varied only at the thousandth and millionth levels, respectively (data not shown). We concluded that undetected sample redundancy in our original GWAS has little impact on our results.

LD analyses and proxy searches were conducted using SNAP software (academic software non-commercial)<sup>24</sup> (CEU 1000 genomes information, 500 kb window and  $r^2 > 0.7$ ).

**Graphic software and other informatics tools.** Regional plots containing meta-GWAS results were generated using LocusZoom (academic software non-commercial).<sup>25</sup> Stage II Manhattan plot was generated using Haploview software<sup>26</sup> (academic software non-commercial; Supplementary Figure S2). Q–Q plots and inflation factor were calculated using SPSS 18.0. A minimal inflation of statistics was observed using fixed effects model meta-analysis ( $\lambda = 1.05$ ). In contrast, a clear deflation was observed for the random effects model ( $\lambda = 0.84$ ), demonstrating that this strategy is over-conservative (Supplementary Figure S3). PC scatterplots were generated using SPSS 18.0.

## RESULTS

The top 1202 SNP ( $P < 0.001$ ) signals obtained in our meta-analysis previously published<sup>9</sup> (Supplementary Figure S1 and Supplementary Table S4) were submitted to the CHARGE consortium for further *in silico* analysis. We received ORs with 95% confidence interval (CI) and risk allele information for 1142/1202 (95%) of the requested markers. The rest of markers (58 SNPs, 5%) were not available in the CHARGE consortium GWAS results, because they did not meet pre-specified quality control criteria; hence these were excluded from our Stage II meta-analysis. Of note, effect estimates were calculated without any modification of published methodologies.<sup>5,9</sup> Then, we combined data from each data set using the meta-analysis tool in PLINK generating a novel SNP list with top signals in terms of effect size and direction. Finally, we mapped the signals using the UCSC genome gateway (<http://genome.ucsc.edu/>) and measured physical distance and LD with known loci with SNAP software. (Supplementary Figure S1 and Supplementary Table S5).

A total of 35 SNPs reached our pre-established threshold for being labeled highly suggestive ( $P < 5 \times 10^{-6}$ ) in the GWAS; these are listed in Supplementary Table S5. Of note, 16 of these 35 SNPs reached our pre-established threshold for GW significance ( $P < 5 \times 10^{-8}$ ), but all signals belonged to known AD loci,

including eight SNPs at the *APOE* locus, *MS4A* gene cluster (four SNPs, the most significant being rs1562990,  $P = 5.05 \times 10^{-10}$ ), *PICALM* (three SNPs, the most significant being rs536841,  $P = 9.67 \times 10^{-10}$ ) and *BIN1* (rs744373,  $P = 2.13 \times 10^{-9}$ ).

The remaining 19 SNPs that reached pre-established highly suggestive *P*-value thresholds also included 12 markers near known AD loci such as *PICALM* (rs2077815), *CLU/APOJ* (rs569214), *CR1* (rs3818361), *BIN1* (rs11685593 and rs7561528) and, again, the *APOE* chromosomal region (7 markers). Of note, another SNP, rs16871253, was located within the *NEDD9* gene. This locus has been previously proposed for AD<sup>27</sup> (Supplementary Table S5).

The list also included seven SNPs, comprising five different chromosomal regions not previously associated with AD (Supplementary Table S5). Specifically, we detected the strongest signal at the *ATP5H/KCTD2* locus (rs11870474,  $P = 2.65 \times 10^{-7}$ ) in a region previously associated with the information processing speed cognitive phenotype.<sup>28</sup> The next strongest signal corresponded to two markers located within the *SLC24A4* gene (rs4406992,  $P = 9.54 \times 10^{-7}$ ; rs2896209,  $P = 4.47 \times 10^{-6}$ ). The third signal was a synonymous cSNP in exon 2 of the cholinergic receptor, nicotinic, alpha 9 gene (rs10022491,  $P = 2.51 \times 10^{-6}$ ). The fourth was an intragenic marker in the utrophin gene (rs2473130,  $P = 3.50 \times 10^{-6}$ ). The last SNP, rs11151137 ( $P = 4.05 \times 10^{-6}$ ), is located in an 800-Kb gene desert at 18q22.1.<sup>21</sup>

We have previously confirmed, using the Fundació ACE data set, all the GWAS-significant loci detected in this study (*APOE*, *MS4A*, *BIN1* and *PICALM*) and also previously known loci classified as highly suggestive in our SNP list (*CR1* and *CLU*).<sup>5,9,29</sup> Consequently, we decided to genotype in the Fundació ACE data set only the five new suggestive loci (at *CHRNA9*, *UTRN*, *SLC24A4*, *ATP5H/KCTD2* and the within the gene desert at chromosome 18) and *NEDD9*. We decided to follow up the *NEDD9* marker because that gene, while previously described as probably associated with AD in one study, has not been confirmed at a genome-wide significance level to date. We achieved a nominally significant signal only for rs11870474 at the *ATP5H/KCTD2* locus (OR = 1.43, 95% CI (1.12–1.83),  $P = 0.0038$ ). The involvement of the other signals in determining risk of AD remains uncertain after our attempted validation and will require further research (Supplementary Table S6).

The rs11870474 signal remained statistically significant even after applying Bonferroni's multiple testing correction for the six markers genotyped during the last stage of our study ( $P = 0.0083$ ) and its effect size remained almost unchanged after covariate adjustments (OR = 1.40, 95% CI (1.08–1.82),  $P = 0.01$ , dominant model). Of note, the magnitude of the effect is quite large and consistent across studies, with all six estimates ranging between 1.31 and 1.85 (see Figure 1). Fixed effects model meta-analysis with all available data sets confirmed this as a novel GWAS

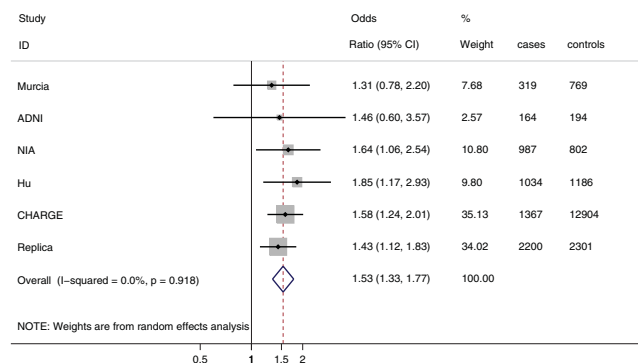


**Figure 1.** Fixed effects model meta-analysis and Forest plot of rs11870474, reporting odds ratio (OR) with 95% confidence interval (CI). ADNI, Alzheimer Disease Neuroimaging Initiative; NIA, National Institute on Aging.



significant locus for AD (Figure 1, OR = 1.533, 95% CI (1.329–1.770),  $P = 5.07 \times 10^{-9}$ ).

## DISCUSSION

We present additional results from a GWAS generated by our group,<sup>9</sup> this time following up on selected top markers in a large independent GWAS generated by the CHARGE consortium.<sup>5</sup> After adding CHARGE information, we confirmed seven different SNPs identical to those previously reported (Supplementary Table S5). However, we cannot consider these independent replications, because some data sets used here overlap with previous studies. We also detected 21 unreported SNPs within previously described loci. Overall, most of the newly identified SNPs are physically close to previously detected signals (300 kb window) (Supplementary Table S7). These new markers might help to refine the association at the previously identified loci and aid the search for functional variants.

Importantly, by merging results of a meta-GWAS conducted by our group, results in the CHARGE consortium data sets and an *in vivo* genotyping comprising 4501 individuals, we were able to detect a novel gene associated with AD risk. Compared with the previous meta-GWAS,<sup>5,7,8</sup> our study had information on an additional 8000 individuals, including the Fundació ACE data set and data derived from Pfizer's GWAS.<sup>18</sup> The larger sample size of 24 227 persons might be one reason why we detected this novel signal, which was not observed in previous GWAS. The *in vivo* genotyping of over 4500 persons was an additional strength of our study design that permitted the signal to reach the pre-established GWAS significance threshold.

As the new locus reaches genome-wide significance only when including the final discovery sample (Stage III), it must still be considered a highly probable finding but not a replicated locus. Independent replications are still required to corroborate this signal. The low frequency of the rs11870474 marker must be taken into account for future replication efforts (Supplementary Table S11). We estimate that a sample size of more than 2450 cases and an equal number of controls will be necessary to reach 80% power to detect its observed effect on AD risk ( $z\text{-alpha} = 1.96$ , case/control ratio = 1, exposure prevalence 3% and OR effect level = 1.53). If we consider adjustment for a possible winner's curse effect,<sup>30</sup> which in fact was observed in the Fundació ACE data set (decreasing observed effect size to 1.43), the number of cases necessary to detect this effect (80% power) could rise to 3660 AD cases. So, it is only by using very large case-control data sets that one can expect to have reasonable power to replicate this observation.

As age/sex data were not available for some data sets, we decided to apply homogeneous criteria to available data sets during Stage I. A potential criticism of our study design emerged from this decision based on our use of young, general population controls, as a proportion of these controls might develop AD as they age. However, although this misclassification might reduce our power to detect an association, it should not create a spurious association. Furthermore, age- and sex-adjusted logistic regression analyses in data sets with covariate data available demonstrated little difference in terms of effect size or statistical significance. (Supplementary Table S10a). Of note, association reported in the CHARGE data set did include age, sex and PC adjustments,<sup>5</sup> and the effect size observed in this data set was remarkably consistent with our Stage I result. A second criticism might be that having controls that are younger than cases might lead to a spurious association with longevity-related genes. However, our discovery sample was largely age-matched for cases and controls and the observed association in the Fundació ACE data set was weaker rather than stronger making it unlikely that the detected locus represents a spurious association with longevity rather than AD. We used this same set of cases and general population controls to successfully replicate relatively 'modest' effects associated with

uncontroversial SNPs located in *PICALM*, *BIN1* and *CLU* loci.<sup>5</sup> We also detected a consistent signal in the *MS4A* gene cluster previously reported by others.<sup>7–9</sup> Notably for these known markers, the observed magnitude of the effect was virtually the same as that reported in the original studies. Furthermore, general population controls have some advantages over neurologically healthy elderly controls, as the latter represent a group of healthy survivors who escaped infectious, cardiovascular and neoplastic diseases. Using such 'hypernormal' controls might jeopardize the generalizability of the risk estimates observed and has been identified as a potential source of bias.<sup>31,32</sup>

Another source of bias could be hidden population stratification affecting the rs11870474 results. We have calculated adjusted effect estimates using two major eigenvectors in three data sets from Stage I with genomewide genotypic data available (Supplementary Table S10b). This analysis revealed little impact of PCs in terms of effect size (OR = 1.49, (1.05–2.13),  $P = 0.02$ ; with three data sets). Of note, the lack of impact of population stratification in our results was also re-enforced by the absence of correlation between PCs and rs11870474 A-allele carrying status (Pearson's determination coefficient ( $r^2$ ) < 1.5%) and the homogenous distribution of carriers observed in multi-dimensional scatterplots representing PC1 and PC2 eigenvectors (Supplementary Figures S5b and S5c). A final model integrating population stratification PCs, age and sex was also applied to the series with these data available (Murcia, ADNI and NIA). Again, little impact on OR estimates was observed (OR = 1.42, (1.003–2.005),  $P = 0.048$ ). In light of these results, we feel that our observations cannot be attributed to population stratification or correlation between the rs11870474 marker and age or sex covariates.

Importantly, rs11870474 genotype was directly genotyped in 15 536 individuals comprising four independent data sets and in half of the CHARGE samples (Supplementary Table S2). Moreover, we obtained validation data for the imputed genotype in 2147 individuals (from the ADNI and NIA). We observed 99% concordance between genotyped and imputed results using PLINK software (data not shown), suggesting that imputation process have been successful for this marker. Furthermore, actual genotyping data were always preferentially selected when available (in the NIA, ADNI and Pfizer GWAS). Case-control differences in allele frequency comparing imputed and non-imputed data sets were almost identical (Supplementary Table S11). These observations suggest a lack of bias during the imputation process.

The potential significance of our finding is also reinforced by the independent previous observation that a locus at the same chromosomal region could also be related to information processing speed, which is an important cognitive function compromised in dementing disorders, and one that might share a genetic background with other complex cognitive traits, such as working memory or abstract reasoning.<sup>28</sup> However, the marker previously associated with information processing speed (rs11077773) only reached a suggestive association  $P$ -value ( $8.33 \times 10^{-6}$ ).<sup>28</sup> Furthermore, in spite of its physical proximity to rs11870474 (it is only 29 kb away), LD among markers is null ( $r^2 = 0.006$ ;  $D' = 1$ ; based on SNAP calculations using 1000 genomes and CEU population). As rs11077773 is not in LD with rs11870474, it is less likely that there is a direct relationship among both observations. Rather, it is probable that these two markers could be tracking different alleles.

The rs11870474 SNP is an intronic non-coding common variant physically located within the second intron of the *KCTD2* gene at 17q25.1 (Figure 2; Supplementary Figure S5). In spite of its small length (33 kb), this locus is located within a region with low LD; there are no large LD blocks in this region and this remains true even when analyzing intragenic markers alone (Supplementary Table S8). This phenomenon makes it difficult to identify proxy signals around rs11870474. However, we did detect a proxy marker, rs12943281, just 716 bp away from rs11870474 ( $r^2 = 0.718$ ,  $D' = 1$ ;  $P = 0.008$ ). These

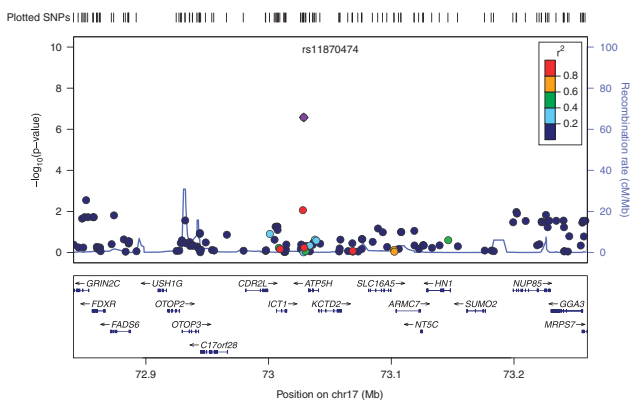


**Figure 2.** Regional Manhattan plot focused on rs11870474 single-nucleotide polymorphism (SNP) with a 250-kb radius around the marker.

results are concordant in terms of effect size and  $p$ -value with rs11870474 during Stage I (OR = 1.59;  $P$  = 0.000359 with five series for rs11870474 and OR = 1.45;  $P$  = 0.008 with four series for rs12943281).

Rs11870474 SNP is located within the *KCTD2* gene intron 2. This gene is a member of the *KCTD* family, which is involved in diverse functions ranging from DNA transcription<sup>33</sup> to degradation of ubiquitinated proteins and proteasome physiology.<sup>34</sup> Other *KCTD* functions are related to voltage-dependent potassium channel function and GABA neurotransmitter receptor B heteromultimeric composition.<sup>35</sup> *KCTD2* expression is ubiquitous according to GeneNote.<sup>36</sup> However, the highest levels of expression are noted in the cerebral cortex and cerebellum.

In spite of these suggestive data, it is important to mention that another transcription unit, named *ATP5H*, is embedded in the third intron of the *KCTD2* gene (Supplementary Figure S4). So, the rs11870474 marker has an alternative candidate gene by position. This *ATP5H* gene encodes ATP synthase, H<sup>+</sup> transporting, mitochondrial F0 (ATP synthase complex V component). Mitochondrial ATP synthase catalyzes ATP synthesis, utilizing an electrochemical gradient of protons across the inner membrane during oxidative phosphorylation. It is composed of two linked multi-subunit complexes: the soluble catalytic core, F1, and the membrane-spanning component, Fo, which comprises the proton channel. The Fo has nine subunits and the *ATP5H* gene encodes the d subunit of the Fo complex.<sup>21</sup> Mutations in other members of the mitochondrial complex V, such as *MTATP6*, result in Leigh syndrome characterized by lactic acidemia, hypotonia, neurodegeneration and MRI (magnetic resonance imaging) brain lesions (OMIM 256000). So, the *ATP5H* gene is related to cell energy production via respiration and its expression is obviously pervasive. The oxidative stress hypothesis for AD, including mitochondrial disturbances, is well documented,<sup>37</sup> and recent studies have confirmed that AD cases have significantly lower expression of the nuclear genes (including the *ATP5H* gene) encoding subunits of the mitochondrial electron transport chain in different regions of the brain.<sup>38,39</sup>

In any case, *KCTD2*, *ATP5H* or both together (as these are probably highly co-regulated loci) are very attractive candidates for AD risk as both are related to fundamental neuronal physiological processes associated with tolerance to hypoxia and other stressors. In fact, potassium conductance alteration and abolition of ATP synthesis are early events necessary to maintain neuronal survival during oxygen deprivation.<sup>40</sup> However, taking into account available data, we cannot decide whether *KCTD2*, *ATP5H*, a common variant altering the transcription of either or even other adjacent genes could explain the observed associations. In fact, a close marker, rs9907177, has been described as an exon-quantitative trait

loci (eQTL) for the growth factor receptor-bound protein 2 (*GRB2*) gene. Interestingly, the *GRB2* gene has been proposed as a candidate for AD. However, this eQTL marker is not associated with LOAD in our series ( $P$  = 0.23, three studies) and its LD with rs11870474 is almost null ( $D'$  = 1,  $r^2$  = 0.037). Therefore, it seems unlikely that rs9907177 can explain the observed association.

We also looked for annotated functional variants around rs11870474 using SNAP software (Supplementary Table S9). We failed to identify any obvious candidate functional variant linked to rs11870474 within a 500-kb radius. Interestingly, this analysis identified *ICT1*, *HNF1* and *SLC16A5* genes as potential candidates explaining our observations. In fact, we observed moderate LD between the detected signal and some intronic SNPs within these genes. The *ICT1* gene was recently reported to be a component of the human mitoribosome essential for cell viability.<sup>41</sup> *HNF1* encodes hemopoietic- and neurological-expressed sequence-1 involved in neuronal regeneration.<sup>42</sup> *SLC16A5* gene is a mono-carboxylate transporter similar to MCT1, which had been involved in mediating axon damage.<sup>43</sup> So, we conclude that other potentially interesting genes are present at this locus. To delineate a more precise hypothesis, further research using next-generation sequencing and detailed functional studies will be necessary.

Finally, it is important to mention that almost all the confirmed new loci identified to date have been unveiled using comprehensive meta-analyses of multiple GWAS and further genotyping on independent series. Given the large numbers of individuals needed to detect this association, it seems likely that we will only be able to discover more markers with international cooperative efforts that incorporate larger GWAS data sets with an increased SNP density.

#### CONFLICT OF INTEREST

LMR, AR and EVT are shareholders of Neocodex. RRL, AGP, JG, JGG, CMR, FJM, JV, JMC, MES, EV and LMR are employed by Neocodex. The other authors declare no conflict of interest.

#### ACKNOWLEDGEMENTS

We thank the patients and controls who participated in this project. This work has been partially funded by the Fundación Alzheimer (Murcia), the Ministerio de Educación y Ciencia (PCT-010000-2007-18), (DEX-580000-2008-4; Gobierno de España), Corporación Tecnológica de Andalucía (08/211) and Agencia IDEA (841318) (Consejería de Innovación, Junta de Andalucía). The Diabetes Research Laboratory, Biomedical Research Foundation. University Hospital Clínico San Carlos has been supported by CIBER de Diabetes y Enfermedades Metabólicas Asociadas (CIBERDEM); CIBERDEM is an ISCIII Project. We are indebted to Trinitat Port-Carbó and her family who are supporting Fundació ACE research programs. We also are indebted to TGEN investigators who provided a free access to genotype data to other researchers via Coriell Biorepositories. The genotypic and associated phenotypic data used in the study, 'Multi-Site Collaborative Study for Genotype-Phenotype Associations in Alzheimer's Disease (GenADA)' were provided by the GlaxoSmithKline, R&D Limited. The data sets used for analyses described in this manuscript were obtained from dbGaP through dbGaP accession number phs000219.v1.p1. Funding support for the 'Genetic Consortium for Late Onset Alzheimer's Disease' was provided through the Division of Neuroscience, NIA. The Genetic Consortium for Late Onset Alzheimer's Disease includes a genome-wide association study funded as part of the Division of Neuroscience, NIA. Assistance with phenotype harmonization and genotype cleaning, as well as with general study coordination, was provided by Genetic Consortium for Late Onset Alzheimer's Disease. The data sets used for analyses described in this manuscript were obtained from dbGaP through dbGaP accession number phs000168.v1.p1. Data collection and sharing for this project was funded by the Alzheimer's Disease Neuroimaging Initiative (ADNI) (National Institutes of Health Grant U01 AG024904). ADNI is funded by the National Institute on Aging, the National Institute of Biomedical Imaging and Bioengineering and through generous contributions from the following: Abbott; Alzheimer's Association; Alzheimer's Drug Discovery Foundation; Amorphix Life Sciences Ltd.; AstraZeneca; Bayer HealthCare; BioClinica, Inc.; Biogen Idec Inc.; Bristol-Myers Squibb Company; Eisai Inc.; Elan Pharmaceuticals Inc.; Eli Lilly and Company; F. Hoffmann-La Roche Ltd and its affiliated company Genentech, Inc.; GE Healthcare; Innogenetics, N.V.; Janssen Alzheimer Immunotherapy Research & Development, LLC; Johnson & Johnson Pharmaceutical Research & Development LLC; Medpace, Inc.; Merck & Co., Inc.; Mesro

Scale Diagnostics, LLC; Novartis Pharmaceuticals Corporation; Pfizer Inc.; Servier; Synarc Inc.; and Takeda Pharmaceutical Company. The Canadian Institutes of Health Research is providing funds to support ADNI clinical sites in Canada. Private sector contributions are facilitated by the Foundation for the National Institutes of Health ([www.fnih.org](http://www.fnih.org)). The grantee organization is the Northern California Institute for Research and Education, and the study is coordinated by the Alzheimer's Disease Cooperative Study at the University of California, San Diego, CA, USA. ADNI data are disseminated by the Laboratory for Neuro Imaging at the University of California, Los Angeles, CA, USA. This research was also supported by NIH Grants P30 AG010129, K01 AG030514 and the Dana Foundation. Fundació ACE collaborates with CIBERNED. The following have contributed to the papers as collaborators: Alejandro Romo, Irene Blanca, Susana Ruiz, Mar Buendía, Fuensanta Noguera-Perea, Emma Rodríguez-Noriega, Evaristo Fernandez-Aranda, Agustina Legaz-García, Laura Vivancos-Moreau, América Morera, Marina Guitart, Susana Lara, Martirio Antequera-Torres, Salvadora Manzanares, Sandra Castaño, Blanca García, Begoña Martínez-Herrada, Sergi Valero.

## REFERENCES

- Ballard C, Gauthier S, Corbett A, Brayne C, Aarsland D, Jones E. Alzheimer's disease. *Lancet* 2011; **377**: 1019–1031.
- Wingo TS, Lah JJ, Levey AI, Cutler DJ. Autosomal recessive causes likely in early-onset Alzheimer disease. *Arch Neurol* 2012; **69**: 59–64.
- Corder EH, Saunders AM, Strittmatter WJ, Schmechel DE, Gaskell PC, Small GW *et al*. Gene dose of apolipoprotein E type 4 allele and the risk of Alzheimer's disease in late onset families. *Science* 1993; **261**: 921–923.
- Harold D, Abraham R, Hollingworth P, Sims R, Gerrish A, Hamshere ML *et al*. Genome-wide association study identifies variants at CLU and PICALM associated with Alzheimer's disease. *Nat Genet* 2009; **41**: 1088–1093.
- Seshadri S, Fitzpatrick AL, Ikram MA, DeStefano AL, Gudnason V, Boada M *et al*. Genome-wide analysis of genetic loci associated with Alzheimer disease. *Jama* 2010; **303**: 1832–1840.
- Lambert JC, Heath S, Even G, Campion D, Sleegers K, Hiltunen M *et al*. Genome-wide association study identifies variants at CLU and CR1 associated with Alzheimer's disease. *Nat Genet* 2009; **41**: 1094–1099.
- Hollingworth P, Harold D, Sims R, Gerrish A, Lambert JC, Carrasquillo MM *et al*. Common variants at ABCA7, MS4A6A/MS4A4E, EPHA1, CD33 and CD2AP are associated with Alzheimer's disease. *Nat Genet* 2011; **43**: 429–435.
- Naj AC, Jun G, Beecham GW, Wang LS, Vardarajan BN, Buross J *et al*. Common variants at MS4A4/MS4A6E, CD2AP, CD33 and EPHA1 are associated with late-onset Alzheimer's disease. *Nat Genet* 2011; **43**: 436–441.
- Antunez C, Boada M, Gonzalez-Perez A, Gayan J, Ramirez-Lorca R, Marin J *et al*. The membrane-spanning 4-domains, subfamily A (MS4A) gene cluster contains a common variant associated with Alzheimer's disease. *Genome Med* 2011; **3**: 33.
- Morgan K. The three new pathways leading to Alzheimer's disease. *Neuropathol Appl Neurobiol* 2011; **37**: 353–357.
- Treusch S, Hamamichi S, Goodman JL, Matlack KE, Chung CY, Baru V *et al*. Functional links between abeta toxicity, endocytic trafficking, and Alzheimer's disease risk factors in yeast. *Science* 2011; **334**: 1241–1245.
- Narayan P, Orte A, Clarke RW, Bolognesi B, Hook S, Ganzinger KA *et al*. The extracellular chaperone clusterin sequesters oligomeric forms of the amyloid-beta(1–40) peptide. *Nat Struct Mol Biol* 2011; **19**: 79–83.
- McKhann G, Drachman D, Folstein M, Katzman R, Price D, Stadlan EM. Clinical diagnosis of Alzheimer's disease: report of the NINCDS-ADRDA Work Group under the auspices of Department of Health and Human Services Task Force on Alzheimer's Disease. *Neurology* 1984; **34**: 939–944.
- Reiman EM, Webster JA, Myers AJ, Hardy J, Dunckley T, Zismann VL *et al*. GAB2 alleles modify Alzheimer's risk in APOE epsilon4 carriers. *Neuron* 2007; **54**: 713–720.
- Mueller SG, Weiner MW, Thal LJ, Petersen RC, Jack CR, Jagust W *et al*. Ways toward an early diagnosis in Alzheimer's disease: the Alzheimer's Disease Neuroimaging Initiative (ADNI). *Alzheimers Dement* 2005; **1**: 55–66.
- Li H, Wetten S, Li St L, Jean PL, Upmanyu R, Surh L *et al*. Candidate single-nucleotide polymorphisms from a genome-wide association study of Alzheimer disease. *Arch Neurol* 2008; **65**: 45–53.
- Wijsman EM, Pankratz ND, Choi Y, Rothstein JH, Faber KM, Cheng R *et al*. Genome-wide association of familial late-onset Alzheimer's disease replicates BIN1 and CLU and nominates CUGBP2 in interaction with APOE. *PLoS Genet* 2011; **7**: e1001308.
- Hu X, Pickering E, Liu YC, Hall S, Fournier H, Katz E *et al*. Meta-analysis for genome-wide association study identifies multiple variants at the BIN1 locus associated with late-onset Alzheimer's disease. *PLoS One* 2011; **6**: e16616.
- Gayan J, Galan JJ, Gonzalez-Perez A, Saez ME, Martinez-Larrad MT, Zabena C *et al*. Genetic structure of the Spanish population. *BMC Genomics* 2010; **11**: 326.
- Ramirez-Lorca R, Boada M, Saez ME, Hernandez I, Mauleon A, Rosende-Roca M *et al*. GAB2 gene does not modify the risk of Alzheimer's disease in Spanish APOE 4 carriers. *J Nutr Health Aging* 2009; **13**: 214–219.
- Kent WJ, Sugnet CW, Furey TS, Roskin KM, Pringle TH, Zahler AM *et al*. The human genome browser at UCSC. *Genome Res* 2002; **12**: 996–1006.
- Purcell S, Neale B, Todd-Brown K, Thomas L, Ferreira MA, Bender D *et al*. PLINK: a tool set for whole-genome association and population-based linkage analyses. *Am J Hum Genet* 2007; **81**: 559–575.
- Abecasis GR, Cherny SS, Cookson WO, Cardon LR. GRR: graphical representation of relationship errors. *Bioinformatics* 2001; **17**: 742–743.
- Johnson AD, Handsaker RE, Pulit SL, Nizzari MM, O'Donnell CJ, de Bakker PI. SNAP: a web-based tool for identification and annotation of proxy SNPs using HapMap. *Bioinformatics* 2008; **24**: 2938–2939.
- Pruim RJ, Welch RP, Sanna S, Teslovich TM, Chines PS, Gliedt TP *et al*. LocusZoom: regional visualization of genome-wide association scan results. *Bioinformatics* 2010; **26**: 2336–2337.
- Barrett JC, Fry B, Maller J, Daly MJ. Haploview: analysis and visualization of LD and haplotype maps. *Bioinformatics* 2005; **21**: 263–265.
- Li Y, Grupe A, Rowland C, Holmans P, Segurado R, Abraham R *et al*. Evidence that common variation in NEDD9 is associated with susceptibility to late-onset Alzheimer's and Parkinson's disease. *Hum Mol Genet* 2008; **17**: 759–767.
- Luciano M, Hansell NK, Lahti J, Davies G, Medland SE, Raikonen K *et al*. Whole genome association scan for genetic polymorphisms influencing information processing speed. *Biol Psychol* 2011; **86**: 193–202.
- Antunez C, Boada M, Lopez-Arrieta J, Moreno-Rey C, Hernandez I, Marin J *et al*. Genetic association of complement receptor 1 polymorphism rs3818361 in Alzheimer's disease. *Alzheimers Dement* 2011; **7**: e124–e129.
- Zhong H, Prentice RL. Correcting 'winner's curse' in odds ratios from genomewide association findings for major complex human diseases. *Genet Epidemiol* 2010; **34**: 78–91.
- Schwartz S, Link BG. The 'well control' artefact in case/control studies of specific psychiatric disorders. *Psychol Med* 1989; **19**: 737–742.
- Schwartz S, Susser E. Genome-wide association studies: does only size matter? *Am J Psychiatry* 2010; **167**: 741–744.
- Ding XF, Luo C, Ren KQ, Zhang J, Zhou JL, Hu X *et al*. Characterization and expression of a human KCTD1 gene containing the BTB domain, which mediates transcriptional repression and homomeric interactions. *DNA Cell Biol* 2008; **27**: 257–265.
- Bayon Y, Trinidad AG, de la Puerta ML, Del Carmen RM, Bogetz J, Rojas A *et al*. KCTD5, a putative substrate adaptor for cullin3 ubiquitin ligases. *FEBS J* 2008; **275**: 3900–3910.
- Schwenk J, Metz M, Zolles G, Turecek R, Fritzius T, Bildl W *et al*. Native GABA(B) receptors are heteromultimers with a family of auxiliary subunits. *Nature* 2010; **465**: 231–235.
- Shklar M, Strichman-Almashanu L, Shmueli O, Shmoish M, Safran M, Lancet D. GeneTide—Terra Incognita Discovery Endeavor: a new transcriptome focused member of the GeneCards/GeneNote suite of databases. *Nucleic Acids Res* 2005; **33**: (Database issue) D556–D561.
- Hirai K, Aliev G, Nunomura A, Fujioka H, Russell RL, Atwood CS *et al*. Mitochondrial abnormalities in Alzheimer's disease. *J Neurosci* 2001; **21**: 3017–3023.
- Terni B, Boada J, Portero-Otin M, Pamplona R, Ferrer I. Mitochondrial ATP-synthase in the entorhinal cortex is a target of oxidative stress at stages I/II of Alzheimer's disease pathology. *Brain Pathol* 2010; **20**: 222–233.
- Liang WS, Reiman EM, Valla J, Dunckley T, Beach TG, Grover A *et al*. Alzheimer's disease is associated with reduced expression of energy metabolism genes in posterior cingulate neurons. *Proc Natl Acad Sci USA* 2008; **105**: 4441–4446.
- Milton SL, Prentice HM. Beyond anoxia: the physiology of metabolic down-regulation and recovery in the anoxia-tolerant turtle. *Comp Biochem Physiol A Mol Integr Physiol* 2007; **147**: 277–290.
- Handa Y, Hikawa Y, Tochio N, Kogure H, Inoue M, Koshiba S *et al*. Solution structure of the catalytic domain of the mitochondrial protein ICT1 that is essential for cell vitality. *J Mol Biol* 2010; **404**: 260–273.
- Zujovic V, Luo D, Baker HV, Lopez MC, Miller KR, Streit WJ *et al*. The facial motor nucleus transcriptional program in response to peripheral nerve injury identifies Hn1 as a regeneration-associated gene. *J Neurosci Res* 2005; **82**: 581–591.
- Lee Y, Morrison BM, Li Y, Lengacher S, Farah MH, Hoffman PN *et al*. Oligodendroglia metabolically support axons and contribute to neurodegeneration. *Nature* 2012; **487**: 443–448.



This work is licensed under a Creative Commons Attribution-NonCommercial-ShareAlike 3.0 Unported License. To view a copy of this license, visit <http://creativecommons.org/licenses/by-nc-sa/3.0/>

Supplementary Information accompanies the paper on the Molecular Psychiatry website (<http://www.nature.com/mp>)